論文

충격시 CFRP 복합재 판의 거동과 충격후 압축강도에 관한 실험적 연구

이정환[*], 공창덕[**+] and Soutis C.[***]

Experimental Investigation on the Behaviour of CFRP Laminated Composites under Impact and Compression After Impact (CAI)

Lee, J.[*], Kong, C.[**+] and Soutis, C.[***]

ABSTRACT

The importance of understanding the response of structural composites to impact and CAI cannot be overstated to develop analytical models for impact damage and CAI strength predictions. This paper presents experimental findings observed from quasi-static lateral load tests, low velocity impact tests, CAI strength and open hole compressive strength tests using 3 mm thick composite plates([45/-45/0/90]$_{3s}$ - IM7/8552). The conclusion is drawn that damage areas for both quasi-static lateral load and impact tests are similar and the curves of several drop weight impacts with varying energy levels(between 5.4 J and 18.7 J) follow the static curve well. In addition, at a given energy the peak force is in good agreement between the static and impact cases. It is identified that the failure behaviour of the specimens from the CAI strength tests was very similar to that observed in laminated plates with open holes under compression loading. The residual strengths are in good agreement with the measured open hole compressive strengths, considering the impact damage site as an equivalent hole. The experimental findings suggest that simple analytical models for the prediction of impact damage area and CAI strength can be developed on the basis of the failure mechanism observed from the experimental tests.

초 록

충격 시나 충격 후 압축 할 때 구조용 복합재의 거동에 대한 중요성은 충격 손상과 충격후압축강도 예측에 대한 해석적 모델을 개발하기 위해 간과될 수 없을 것이다. 본 연구는 3mm두께의 [45/-45/0/90]$_{3s}$ - IM7/8552복합재판들을 이용하여 준정적횡하중시험, 저속충격시험, 충격후압축강도시험 및 구멍이 있는 시편의 압축강도시험 등을 수행한 후 이로부터 발견된 결과들을 제시하였다. 준정적횡하중과 충격하중시험에서 발생한 손상면적들이 서로 유사하며, 또한 5.4 J부터 18.7 J 까지의 다양한 에너지준위들을 가진 낙하충격 시험 곡선들과 정적시험 곡선들도 서로 유사하다는 결론을 얻었으며, 이때 주어진 에너지 준위에서 정적 과 충격시의 최대하중 값들이 잘 일치한다는 사실을 확인 하였다. 충격후 압축시험에 의한 시편들의 파괴거동이 압축하중하의 구멍이 있는 적층판에서 관찰된 파괴거동과 매우 유사하다는 사실도 확인 되었다. 충격손상 후 잔류강도는 충격손상 등가구멍이 있는 경우의 시편에서 측정된 압축 강도와 잘 일치하였다. 이와 같은 실험적 연구 결과들은 충격손상면적과 충격후압축강도의 예측에 대한 단순한 해석모델들이 이들 시험결과들로부터 관찰된 파괴기구를 기초로 하여 개발될 수 있음을 제시하고 있다.

Key Words: 준정적횡하중(Quasi-static lateral load), 저속충격(Low velocity impact), 충격후압축강도(CAI), 구멍이 있는 경우 압축강도(Open hole compressive strength)

 * Department of Aeronautics, Imperial College London, UK
**+ Department of Aerospace, Chosun University, Korea, 교신저자(E-mail:cdgong@mail.chosun.ac.kr)
*** School of Aerospace Engineering, Sheffield University, UK

1. Introduction

The damage caused to carbon fibre composite structures by low velocity impact, and the resulting reduction in compression after impact(CAI) strength has been well known for many years[1,2] and is of particular concern to the aerospace industry, both military and civil. Typically the loss in strength may be up to 60 % of the undamaged value and traditionally industrial designers cope with this by limiting compressive strains to the range of 0.3 % to 0.4 %(3000 to 4000 $\mu\varepsilon$). Provided buckling is inhibited by good design of the compression panels the material is capable of withstanding more than double these values.

An impact damage site in a composite laminate contains delaminations, fibre fracture and matrix cracking. A model to predict the damage area taking into account all these factors would be complex and take considerable time and funding to develop. It was recognised that the problem could be simplified by making some assumptions about the nature of the impact damage.

In the present work, experimental findings are presented to develop simple analytical models for impact damage and CAI strength predictions based on the failure mechanism observed from the quasi-static lateral load tests, impact tests and compression-after-impact(CAI) tests in future work. It will be identified that the low velocity impact can be modeled as a quasi-static lateral load problem[3] and provide a measure of how good an approximation we have, comparing the quasi-static response with dynamic response. In addition, the failure behaviour of composite specimens under static compressive loading after impact will be compared to the compressive behaviour of open hole specimens.

2. Experimental

2.1 Materials and Lay-up

The material is IM7/8552 supplied by Hexel Composite Ltd. as a roll of pre-impregnated tape of epoxy matrix(8552) reinforced by continuous intermediate modulus unidirectional carbon fibres(IM7). The roll was 350 mm wide and about 0.125 mm thick. The prepreg was cut into 500 mm wide by 500 mm long sheets using a metal template and laid up in the quasi-isotropic stacking sequence([45/-45/0/90]$_{3s}$) giving a total thickness of about 3mm thickness. The in-plane stiffness and strength of the IM7/8552 unidirectional laminate are

given in Table 1. These parameters were obtained by BAE system from material strength tests.

Table 1   Stiffness and strength properties for the IM7/8552 composite system

E_{11}, GPa	155	$\sigma_{11T}/\sigma_{11C}$, MPa	2400/1300
E_{22}, GPa	10	$\sigma_{22T}/\sigma_{22C}$, MPa	50/250
G_{12}, GPa	4.6	τ_{12}, MPa	85
ν_{12}	0.3	-	-

($\sigma_{11T}/\sigma_{11C}$ are longitudinal tensile and compressive strength and $\sigma_{22T}/\sigma_{22C}$ are transverse tensile and compressive strength)

2.2 Quasi-static Lateral Load Tests

Quasi-static lateral load test was carried out to measure the maximum deflection at the centre of a circular plate and strain data on the top and bottom surface of the plate. The loading was transferred from the cross-head to the plates through a flat nose with a diameter of 12 mm, using a screw-driven Zwick 1488 universal testing machine with a load capacity of 200 kN. The cross-head speed used in this study was 0.5 mm per minute. For measuring the central deflection of the plate, an LVDT displacement transducer was used. The experimental setup and specimen jig are shown in Fig. 1.
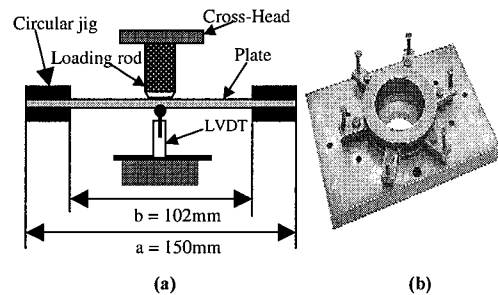

Fig. 1   (a) Setup of quasi-static lateral load tests with (b) a jig on circular plates.

2.3 Low Velocity Impact Tests

Circular plates cut from a 3 mm thick IM7/8552 multidirectional laminate([45/-45/0/90]$_{3s}$) are subjected to low-velocity impact using a drop-weight test rig with two different impactor masses(1.58 kg and 5.52 kg). The specimen dimension and jig are the same as those used in the quasi-static lateral load test(see Fig. 1). The test setup is shown schematically in Fig. 2. An impactor with a flat-ended
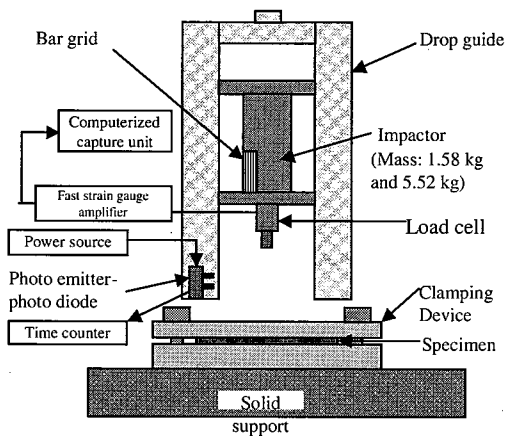
Fig. 2 Schematic diagram of the impact test rig.

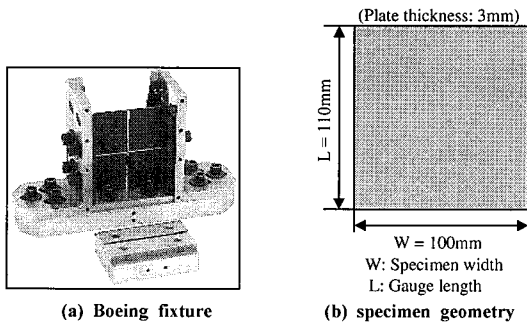(a) Boeing fixture   (b) specimen geometry

Fig. 3 (a) Boeing fixture and (b) specimen geometry for CAI strength test.

nose of 12 mm in diameter is instrumented with a strain-gauged load cell providing a record of force-time history. The impactor was dropped at the centre of the specimen from a selected height. After impact, the damage of each specimen was visually inspected for surface damage. The examination of interior damage was carried out using primarily ultrasonic C-scan and occasionally by X-ray radiography.

2.4 CAI Strength Tests

Post-impact tests were performed to determine CAI strengths for a range of impact levels, which induce fibre damage. For the test various methods have been used[11]. A side-supported fixture developed by the Boeing Company for compression residual strength tests was used in the current study(see Fig. 3). The fixture was placed on a fixed compression platen in a screw-driven Zwick 1488 universal testing machine with a load capacity of 200 kN. The specimens were loaded until failure at a rate of 0.5 mm/min.

When performing compression of the impacted specimens, several plain specimens which had not been impacted were tested in compression to provide baseline undamaged specimen data with the modified ICSTM fixture used in the static compressive test[16]. The dimensions of the plain specimen are 30 mm × 30 mm in gauge length and specimen width. In addition, open hole compression tests were carried out in accordance with the specimen dimensions for CAI test. Hole diameters obtained from X-ray radiographs by measuring the size of the darkest region of impacted specimens were used (see Figure 7 (b)). This data would effectively show what the compressive strength would be if the stiffness property of the damaged region is zero.

3. Results and Discussion

3.1 Quasi-static Lateral Load tests

Clamped circular specimens were loaded at the centre by a normal load. Fig. 4 shows a typical force-deflection curve for a circular plate, where the deflection was measured by an LVDT at the centre of the plate. During the testing, the first load drop was observed around 10 kN with an audible acoustic event(see Fig. 4). The force gradually recovered up to around 11.5 kN. Then the load fell again but did not recover up to 11.5 kN. This clearly indicates the reaching of a maximum contact force once fibre fracture occurs and also illustrates the large amount of energy that is lost as the fibre fracture and the loading rod penetrates the plate.

A visual and C-scan inspection of the specimens were carried out to examine specimen damage from the applied load, 6 kN to 11.5 kN with the increment of 1 kN. No visual damage was found at the top and bottom surface of
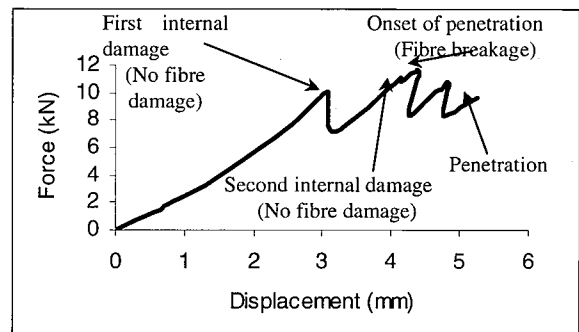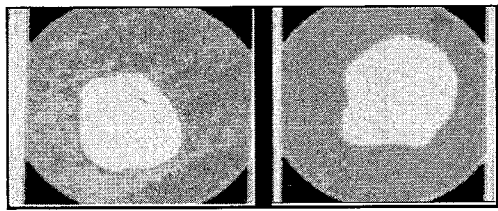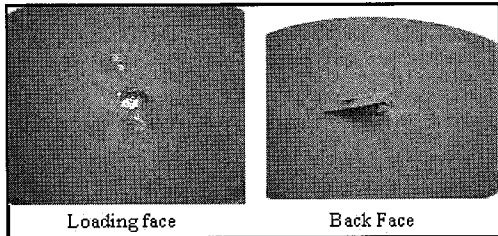

Fig. 4 Typical static force-deflection curve for the circular plate with a diameter of 102 mm([45/-45/0/90]$_{3s}$ - IM7/8552).

(a) C-scan images at 10 kN (b) C-scan images at 11.5 kN

Loading face　　　　　Back Face

(c) Photograph at loading face and back face in the specimen

Fig. 5　Static damages taken by C-scan and photographs([45/-45/0/90]$_{3s}$ - IM7/8552).

(a)

(b)

Fig. 6　(a) Force-time and (b) force-displacement curves for representative impacts on quasi-isotropic([45/-45/0/90]$_{3s}$) IM7/8552 laminates.
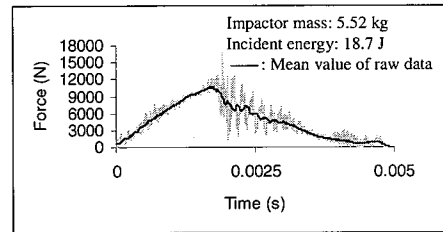
the specimen up to an applied load of 10 kN. Significant internal damage was, however, detected from C-scan examination with the applied load, 10 kN, as shown in Fig. 5 (a). Much severer damage was observed around 11.5 kN just prior to ultimate failure which is caused by tensile fibre fracture on the back face of the specimen allowing the flat nose loading rod to eventually penetrate the specimen(See Fig. 5 (b) and (c)).
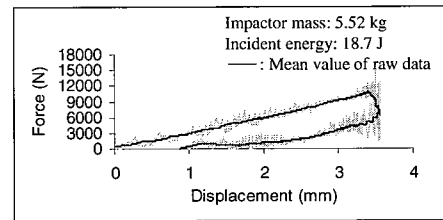
3.2 Low Velocity Impact Tests

Two sets of impact tests were performed with different impactor masses. Firstly, 3 mm thick circular plates of the IM7/8552 system were subjected to low-velocity impact with the impactor mass of 1.58 kg under the range of incident energy between 5 J and 11 J. Secondly, impact test was carried out with the impactor mass of 5.52 kg under the range of incident energy between 16 J and 19 J.

Fig. 6 (a) shows a typical force versus time history for impact with damage. It is for a 3 mm thick circular plate with clamped edges under incident energy of 18.7 J(impactor mass: 5.52 kg). Fig. 6 (a) exhibits fluctuation around the peak force, making it possible to identify the onset of damage. A slower recovery also indicates a decrease in the structural stiffness due to damage.

By integrating the force-time curve, the displacement can be calculated. On the base of the displacement data, the force-displacement curves can be plotted as shown in Fig. 6 (b). Fig. 6 (b) show the force-displacement curves for the

tests of Fig. 6 (a). Once the impactor energy is exhausted, the load starts to drop and reaches zero at a permanent displacement value as shown in Fig. 6 (b). These force-displacement curves will be compared with the curve measured from the quasi-static lateral load test in the next section.

After drop tests all the circular specimens were inspected using ultrasonic C-scan to assess the extent of their internal damage caused. The specimens subjected to low-velocity impact with the impactor mass of 1.58 kg did not show any damage. However the specimens impacted with the impactor mass of 5.52 kg show significant internal damage with or without visible damage on the specimen surface depending on the amount of incident energy. Figure 7 (a) and (b) present the impact damage of the specimen for the test of Fig. 6 (incident energy: 18.7 J) using ultrasonic C-scan and X-ray radiograph, respectively.

The intensity of the dark region shown in Fig. 7 (b) is a measure of the extent of severe damage in the specimen including matrix cracking, delamination, fibre splitting and fibre fracture developed; sectioning/polishing and de-ply studies[5,6] revealed that in the very dark area fibre breakage and delaminations exist in almost all interfaces through the thickness of the laminate. The lighter region in Fig. 7 (b) corresponds to the splitting and delamination of the back face rather than internal damage. The circled dark region will be used as the replacement of the impact damage with an equivalent open hole for the compression after impact(CAI)
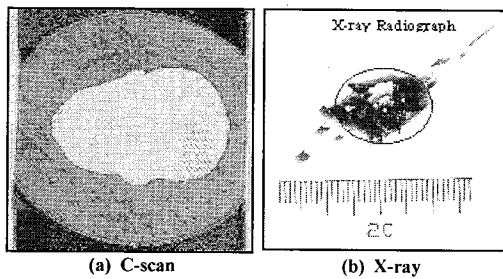
(a) C-scan   (b) X-ray

Fig. 7   Impact damage of a quasi-isotropic([45/-45/0/90]₃ₛ) IM7/8552 laminate, taken from (a) C-scan and (b) X-ray radiograph with an incident energy of 18.7 J.
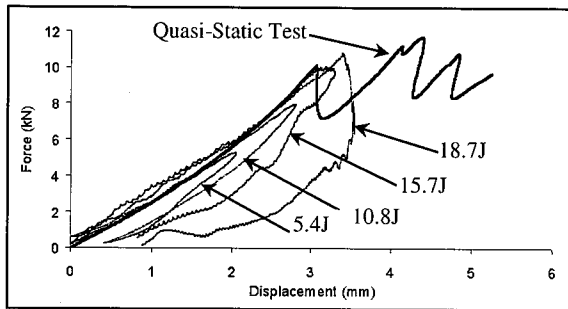

Fig. 8   Comparison of the force-displacement curves of impact tests at increasing energy levels(between the curve from a continuous quasi-static lateral loading test for circular plates of a 102mm diameter([45/-45/0/90]₃ₛ - IM7/8552).

Fig. 9   Peak contact force against impact energy for tests on clamped circular plates of 102 mm diameter([45/-45/0/90]₃ₛ - IM7/8552).

(a) Quasi-static test   (b) Impact Test

Fig. 10   C-scan images taken from (a) static and (b) impact test at a peak force of approximately 10 kN for the circular plates of 102 mm diameter([45/-45/0/90]₃ₛ - IM7/8552).

strength prediction and compared to the estimated impact damage area in future study.

3.3 Comparison of Quasi-Static Lateral Load and Low Velocity Impact Test Results

Impact events that involve a high mass impacting a relatively small target at low velocities can usually be thought of as quasi-static events[3,4,7,8,9,10]. The most direct way to determine whether an impact event can be considered quasi-static is to compare two cases experimentally. Fig. 8 shows the static and dynamic responses of 3 mm thick quasi-isotropic IM7/8552 panels. In the figure the force-displacement curves of several drop weight impacts with varying energy levels(between 5.4 J and 18.7 J) are superposed on a static deflection test. The quasi-static deflection test was carried to complete perforation of the specimen. The loading paths of all the impact events follow the static curve quite well. The difference between the static and dynamic responses shown in Fig. 8 is within the scatter of the data.

In Fig. 9, the quasi-static response is again indicated for the same static and impact events as shown in Fig. 8, where peak contact f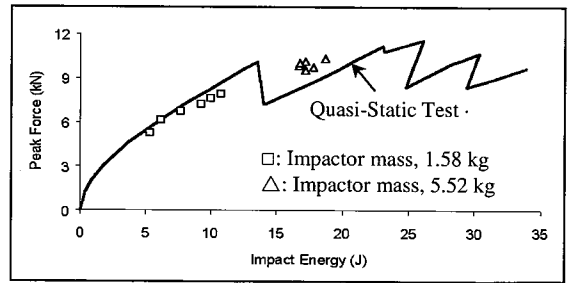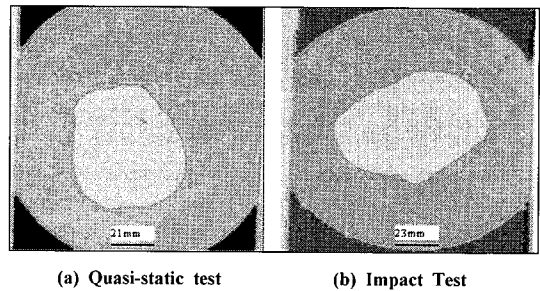orce for each test is plotted as a function of impact energy. This is compared with the force against energy absorbed for a quasi-static test, the energy absorbed being calculated by integrating the area under the load-displacement curve. It can clearly be seen that at a given energy the peak force is in good agreement between the static and impact cases.

The impact data is in good agreement with the static curve for impact energies of 15 J - 17 J where interior damage is only detected without visual damage on both surfaces of the plate(see Fig. 10). At higher impact energy of 18.7 J(peak force 10.3 kN), the data are also in reasonable agreement with the quasi-static curve(peak force 11.5 kN) where fibre fracture on the bottom face is clearly visible. This is a very good indication that the damage mechanism, from the point at which damage first initiates to the point that the indenter has penetrated the plate, are similar to the quasi-static and impact loading considered in this study. In addition, the good agreement between the impact peak forces and the static load as a function of impact energy would suggest that the damage areas should be in good agreement between the static and dynamic test cases(see Fig. 10). Fig. 10 shows C-scan images taken from the static and impact test at a peak force of approximately 10 kN. It can be seen that damage areas are similar regardless of the test method.
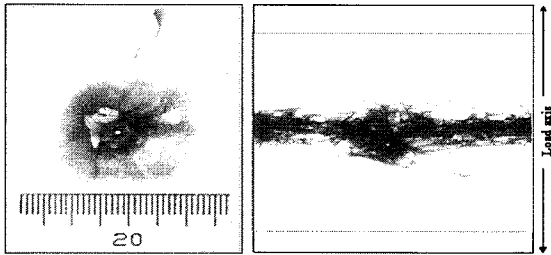
Fig. 11 Impacted CAI specimen (a) before and (b) after CAI strength test showing compression failure with a kink-band shear([45/-45/0/90]$_{3s}$ - IM7/8552).

Table 2 Impact, CAI and OHC test results([45/-45/0/90]$_{3s}$ - IM7/8552)

Impact Results		Incident Energy (J)	17.8	18.2	18.7
		Peak Force (kN)	9.7	10.1	10.3
Compressive Failure Strengths (MPa)		a/W	0.13	0.17	0.18
		CAI	280	243	242
		Open Hole	271	-	229
		Unimpacted		685	

(a = width of impact damaged area; W = laminate width, 100mm)

3.4 CAI Strength Tests

Each circular plate was impacted with a known energy level of between 5 and 19 J. An energy level between 5 and 16.8 J was too insignificant to encourage the test-piece to fail at the impact site. Most data for fibre breakage has been obtained between 17 and 19 J.

During the CAI testing, clear cracking sounds were heard around the damaged area due to matrix cracking, fibe-matrix debonding, delamination and fibre breakage. As the applied load is increased, damage in the form of local buckling like a crack grows laterally from the impact damage region. In addition, delaminated regions continued to propagate, first in short discrete increments and then rapidly at the failure load. Examination of the failed specimens removed from the test fixture confirmed that the local delaminations extended completely across the specimen width but extended only a short distance in the axial direction with a kink shear band through the laminate thickness (see Fig. 11 (b)). This pattern of damage growth[12-15] is similar to that observed in specimens with open holes under uniaxial compression as described in Refernce16. Fig. 11 (a) and (b) show a typical impacted specimen before and after CAI strength test taken by X-ray radiography. Specimen failure after CAI strength test shows fibre kink band shear through its thickness.

The residual compressive strengths and impact results are summarized in Table 2. In the table the extent of damage caused by the impact was observed by X-ray radiographs as shown in Fig. 7 (b). The compressive strengths of unimpacted plain specimens and open hole specimens measured to provide reference values are also included in the table. For the open hole specimens, the observed impact damage is replaced with an equivalent open hole. It can be seen that the residual strengths are reduced up to 64 % of the unimpacted compressive strength between an energy level of 17.8 J and 18.7 J. In the case of an equivalent open hole specimens, the failure strengths (OHC) are in good agreement with those of the residual strengths (CAI), the difference is less than 10 %. Soutis et. al.[12,15,17] have also performed this strategy, which considers impact damage site as an equivalent hole to predict the CAI strength of different composite systems and lay-ups. They used damage width measured from X-ray radiographs for the prediction. The theoretical predictions are in a good agreement with the experimental measurements.

4. Concluding Remarks

A quasi-static and dynamic series of tests were performed using 3 mm thick circular plates([45/-45/0/90]$_{3s}$ - IM7/8552) with a flat-ended impactor to compare the static response with the dynamic response and identify damage patterns between them. In the dynamic test, two different impactor masses were used with varying impact energy level, i.e. impactor mass of 1.58 kg under the range of incident energy between 5 J and 11 J and 5.52 kg under the range of incident energy between 16 J and 19 J.

During the quasi-static and impact testing, the development of damage was monitored using C-scan and X-ray radiography. Significant interior damage was detected at the similar applied peak load, 10 kN from the quasi-static test and 9.8 kN from the impact test prior to initiation of tensile fibre damage on the tensile face of the plates under the indenter. In addition, it has been found that damage areas for both tests are similar(see Fig. 10). From the investigation of damage patterns performed by Sjoblem, P. and Hartness, J.[7] using microscopy, it is identified that both the statically tested and the impacted circular plate specimens have similar conical shape of damage under the indenter.

In comparison of the force-displacement responses obtained from both tests, it was confirmed that the curves of several

drop weight impacts with varying energy levels(between 5.4 J and 18.7 J) follow the static curve quite well(see Fig. 8). In addition, the peak contact force-impact energy graph plotted to be compared with the force against energy absorbed for a static test(see Figure 9) showed that at a given energy the peak force is in good agreement between the static and impact cases.

Finally CAI tests were conducted to determine residual compressive strength of the plates impacted at an energy level between 17 J and 19 J. The failure behaviour of the specimens was very similar to that observed in laminated plates with open holes under compression loading. The residual strengths between an impact energy level of 17 J and 19 J varied from 280 MPa to 242 MPa and reduced to 64 % of the unimpacted compressive strength(685 MPa). The measured open hole compressive strengths were in good agreement with the residual strengths, considering the impact damage site as an equivalent hole. The size of the hole was determined from X-radiograph images.

The experimental results above indicate that the low velocity impact response for the plates tested in this study is close to quasi-static behaviour. This means that inertia effects are negligible and hence the plate response is the fundamental, or statically deflected, mode. It is also indicated that impact damage site for CAI strength can be modelled as an equivalent hole. On the basis of these experimental findings, simple analytical models will be developed to predict impact damage area, reduced elastic properties due to the impact load and CAI strength in future work. The results obtained in this study will be compared to the predict results.

Acknowledgement

References

1) Whitehead R.S., "ICAF National Review," *Pisa*, May, 1985, pp. 10-26.
2) Greszczuck L.B., "Damage in Composite Panels due to Low Velocity Impact," *Impact Dynamics*, Ed. Zukas Z.A. J. Wiley, 1982.
3) Dahsin, L, "Impact-induced Delamination - a View of Bending Stiffness Mismatching," *Journal of Composite Materials*, 1988, Vol. 22 (July), pp. 674-692.
4) Zhou, G and Davies, G. A. O., "Impact Response of Thick Class Fibre Reinforced Polyester Laminates," *International Journal of Impact Engineering*, 1995, Vol. 16, No. 3, pp. 357-374
5) Guynn, E. G. and O'brien, T. K., "The Influence of Lay-up and Thickness on Composite Impact Damage and Compression Strength," *Proc. 26th Structures*, Structural Dynamics, Materials Conf., Orlando, FL, April, 1985, pp. 187-196.
6) Hitchen, S. A. and Kemp, R. M., "The Effect of Stacking Sequence and Layer Thickness on the Compressive Behaviour of Carbon Composite Materials: Impact Damage and Compression after Impact," *Technical Report 94003*, Defence Research Agency, Farnborough, 1994.
7) Sjoblem, P. O. and Hartness, J. T., "On Low-Velocity Impact Testing of Composite Materials," *Journal of Composite Materials*, Vol. 22, Jan., 1988, pp. 30-52.
8) Delfosse, D and Poursartip, A, "Energy-Based Approach to Impact Damage in CFRP Laminates," *Composites Part A*, Vol. 28, No. 7, 1997, pp. 647-655.
9) Watson, S. A., "The Modelling of Impact Damage in Kevlar-Reinforced Epoxy Composite Structures," *PhD Thesis, University of London*, November, 1994.
10) Hou, J., "Assesment of Low Velocity Impact Induced Damage on Laminated Composite Plates," *PhD Thesis*, University of Reading, September, 1998.
11) Hodgkinson, J., "Mechanical Testing of Advanced Fibre Composites," *Woodhead Publishing Ltd*, 2000.
12) Soutis, C. and Curtis, P. T., "Prediction of The Post-Impact Compressive Strength of CFRP Laminated Composites," *Composite Science and Technology*, Vol. 56, No. 6, 1996, pp. 677-684.
13) Zhou, G., "Effect of Impact Damage on Residual Compressive Strength of Glass-Fibre Reinforced Polyester (GFRP) Laminates," *Composite Structures*, Vol. 35, No. 2, 1996, pp. 171-181.
14) Davies, G. A. O., Hitchings, D. and Zhou, G, "Impact Damage and Residual Strengths of Woven Fabric Glass/Polyester Laminates," *Composites Part A*, Vol. 27, No. 12, 1996, pp. 1147-1156.
15) Hawyes, V. J., Curtis, P. T., and Soutis, C., "Effect of Impact Damage on The Compressive Response of

Composite Laminates," *Composites Part A,* Vol. 32, No. 9, 2001, pp. 1263-1270.

16) Soutis, C., Lee. J. and Kong, C., "Size Effect on Compressive Strength of T300/924C Carbon Fibre-Epoxy Laminates," *Plastics, Rubber and Composites,* Vol. 31, No. 8, 2002, pp. 364-370.

17) Soutis, C., Smith, F. C. and Matthews, F. L., "Predicting the Compressive Engineering Performance of Carbon Fibre-Reinforced Plastics," *Composite Part A,* Vol. 31, No. 6, 2000, pp. 531-536.